25th ABCM International Congress of Mechanical Engineering
October 20-25, 2019, Uberlândia, MG, Brazil

COB-2019-1808
THE EFFECT OF HEAT TREATMENT ABOUT THE DUCTILITY AND THE STRAIN-HARDENING EXPONENT FOR THE AL-CU-FE-ZR ALLOY

Vinicius Silva dos Reis[1]
Beatriz Seabra Melo [1]
e-mail: beatrizseabrak@hotmail.com
e-mail: viniciusreis11@hotmail.com

Gregory de Oliveira Miranda[1]
e-mail: eng.marcusw@gmail.com

Clóvis Iarlande Oliveira Santana[1]
e-mail: clovis.mecanica@hotmail.com

Carlos Vinícius de Paes Santos
e-mail: carlosviniciusdepaessantos@gmail.com

Marcos Felipe Macêdo Cardoso[1]
e-mail: eng.marcusw@gmail.com

José Maria do Vale Quaresma[1]
e-mail: quaresma@fem.unicamp.br

UFPA – Federal University of Pará – Rua Augusto Corrêa, 01 – Guamá. CEP 66075-110. Belém – Pará – Brazil[1]

Abstract. *The aim work is the influence of the heat treatment on the Strain-Hardening Exponent [η] of the Al-0.05%Cu-0.40%Fe-0.22%Zr alloy. The ingots were obtained by casting in a U-shape metallic mold, machined and separated into two lots: the first is the material without heat treatment; the second was heat treated for 2 hours at 150°C. Subsequently, the samples from both lots were cold rolled up to the [4.0, 3.8, 3.0, 2.7] mm diameters. The wires were subjected to the resistivity test and tensile test, in which it was determined the electrical and mechanical characteristics, respectively. The values of Strain-Hardening Exponent [η] were obtained by the Hollomon method, applying data from the tensile test. It was analyzed the variation of [η] compared to the UTS values, and correlated to the ductility evaluation, using the elongation [δ] and dimples ratio [9], obtained by quantitative metallography applied to photomicrographs of the wire fractures. It was observed that the increasing values of [η], presented by the heat-treated specimens, showed a relation with increasing ductility of the material.*

Keywords: *Al-Zr alloys, Heat treatment, Mechanical characterization, Strain-hardening Exponent and Ductility.*

1. INTRODUCTION

Electricity consumption can be considered an indicator of socioeconomic development for any nation, according to Brazil, 2010. Since energy demand is seen in both industrial, commercial and service growth, as well as the ability of the population to purchase goods and services. This is evidenced by Sorrell, 2015. During the last decades, there has been an increase in the demand for electric, industrial and domestic energy. Meeting this demand generates numerous problems, such as manufacturing and building new high voltage cables with new materials.

According to Régis et al., 1999 a conductor with heat resistant aluminum can be used in a continuous working regime at temperatures of up to 150ºC without deterioration of the mechanical characteristics, such as: traction, stretching and hardness.

The studies of Knipling et al., 2007 and Çadırlı et al., 2015 on heat treated Al alloys in which precipitation of Zr occurs as the compound Al3Zr, which shows the influence of these precipitates on the mechanical and electrical properties of the alloys analyzed.

According to literature Polmear et al., 2017 during plastic deformation of metals and alloys, the density of disagreements increases when the generation and multiplication is higher than the annihilation caused by dynamic

recovery, forming tangles of discordance, cells and subgrain contours. The average distance between the sliding planes decreases, leading to increased resistance and, consequently, material hardening. This definition applies to the emergence of mechanical changes in materials, such as the Portevin-Le Chatelier [PLC] effect. This effect is found in various aluminum alloys.

Moreover, literatures such as Mccormick, 1972, Soare and Curtin, 2008 and Hu et al., 2011 define that the physical origin of the PLC effect is a process called "Dynamic Agin". It consists of the interaction between moving disagreements and second phase particles, characterized by serrations on Stress [σ] x Strain [ε]curve.

The present study aims to assess the effect of heat treatment 150°C for 2 hours on the work hardening coefficient and mechanical alloy of Al-0.05% Cu-0.40% Fe-0.22% Zr for application to transmission and distribution of electricity through wires and cables. Thus, evaluating the ductility of the alloy by means of the correlation between the elongation [δ], the dimples Ratio [θ] and the strain-hardening exponent [η].

2. MATERIALS AND METHODS

The alloy was obtained by direct casting of the Al-EC alloy, called Aluminum Electroconductor. The preparation of the base alloy was performed from the additions of 0.05% Cu and [0.35 to 0.45]% Fe, percentage by weight, and modified with the content of 0.22% Zr in proportions to obtain the desired chemical composition.

The alloy was cooled in “U” metal mold, this mold is seen in Figure 1.a, and after demoulding the ingots, Figure 1.b were machined to diameter 18.5 mm, separating the profiles into two batches: in the first, in the molten condition and the second subjected to 150 °C heat treatment, based on the work of Kamizono, 2014, for a period of 2 hours. The untreated and heat treated samples are referred to as [STT] and [TT 150°C/2h]. The treat and untreated lots were submitted to cold rolling, generating the samples used in the tests in the form of wires in the diameters [4.0, 3.8, 3.0, 2.7] mm.

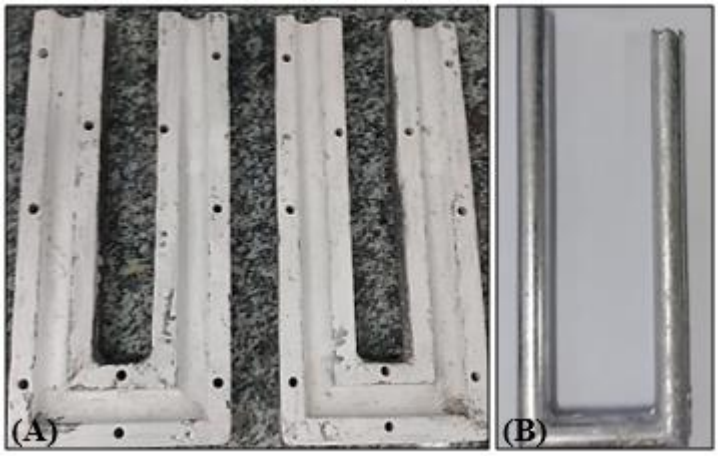

Figure 1. “U” type mold. (a) Open ingot mold; (b) Material obtained after casting. Available from: GPEMat file.

The proof bodies were submitted to the tensile test in order to evaluate the mechanical properties of the wires. The tests followed the standards of the norm for electrical cables NBR 6810, in samples with 20 cm of length.

The data obtained from the traction test in the shape of worksheets are used to plot the curve Stress [σ] x Strain [ε]. Then, the material flow limit is determined by the offset method, for [ε] = 0.2%. Considering the linearization of the Hollomon equation and the ASTM E646-16 standard, the Strain-hardening Exponent was calculated.

The schematicization of the region used for photomicrographic characterization is shown in Figure 2, for the analysis of the fracture seen in Figure 2c, scanning electron microscopy (SEM) was used and with the aid of MOTIC IMAGES PLUS 2.0 software, which assists in the reading of the fractures. dimensions and shapes of the wells by calibrating with the scale of the image itself. The design of the wells followed the proposed method to obtain the Ratio [θ] between the readings of the wells dimensions, used in specialized literature. This method was adaptation of the ASTM E112-13 standard and the studies by Narayanasamy et al., 2008 and Nagakrishna et al., 2010.

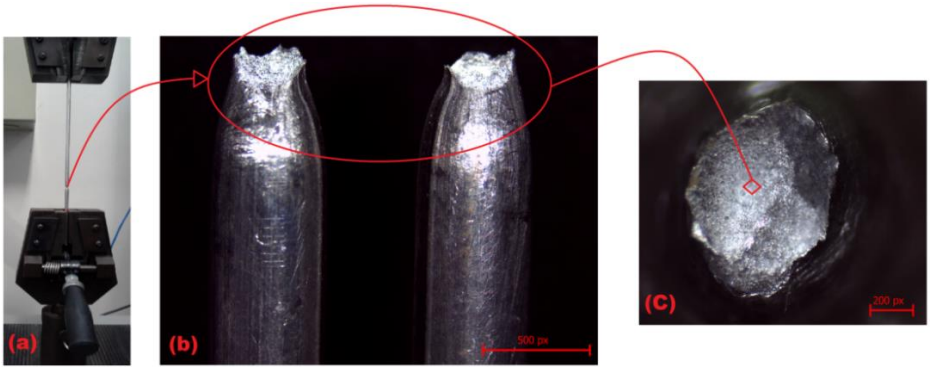

Figure 2. (a) Traction specimen, (b) identification of SEM analysis regions, (c) fracture of the test wire. Available from: GPEMat file.

3. RESULTS END DISCUSSIONS

3.1. Chermical composition

The result of the chemical composition of the material produced, presented in Table 1, indicating that all the procedures were carried out in an appropriate way and the chemical composition obtained did not suffer great fluctuations, in agreement with the scope of this work. The composition reading was obtained from optical spectrometer analysis.

Table 1. Chemical composition of the base alloy after solidification.

Alloy	**Alloys Elements [%Wt]**		
Al-0.05Cu-[0.35-0.45]Fe-0.22Zr	Cu	Fe	Zr
	0.051	0.397	0.218

3.2. Evaluation of the alloy ductility

Alloy ductility analysis was performed previously in studies proposed by Sharma et al. (2009), in which the ductility was measured indirectly from the Stretching and quantitative metallographic aspects of images of the fractures generated by SEM without correlation with the values of [η]. The differential of the present work is precisely the development of the studies through the correlation between the variations of these properties, seeking possible answers for the modifications that the heat treatment provoked in the structure of the metallic alloy.

3.2.1. Alloy without heat treatment

The results in Table 2 and Figure 3 relate the Elongation [δ], Strain Hardening Coefficient [η] and Dimples Ratio [θ] values for the alloy in STT condition for all diameters.

Table 2. (a) Elongation [δ]; (b) Strain Hardening Coefficient [η]; (c) Dimples Ratio [θ]for Al-0.05% Cu- [0.35-0.45]% Fe-0.22% Zr STT, for all diameters.

Al-0.05% Cu- [0.35-0.45]% Fe-0.22% Zr STT(1)			
Diameter wires [mm]	**Elongation [δ]**	**Strain Hardening Coefficient [η]**	**Dimples Ratio [ϑ]**
2.7	3.81	0.09	1.23
3.0	4.67	0.10	1.25
3.8	5.02	0.13	1.28
4.0	5.15	0.15	1.29

(1) Without heat treatment

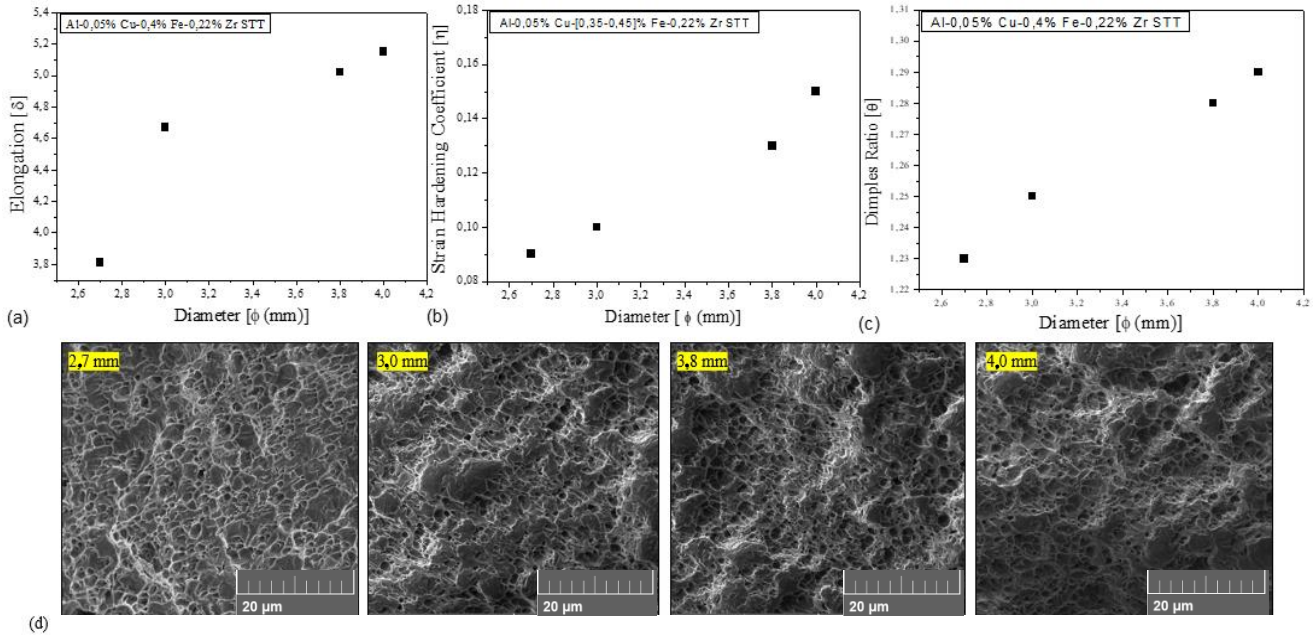

Figure 3. Ductility evaluation: (a) Elongation [δ]; (b) Strain Hardening Coefficient [η]; (c) Dimples Ratio [θ], for the alloy Al-0.05% Cu- [0.35-0.45]% Fe-0.22% Zr STT, (d) for all diameters and associated with photomicrographs of the fractures for the diameter wires. Available from: GPEMat file.

3.2.2. Alloy with heat treatment

Table 3 and Figure 4 show the the Elongation [δ], Strain Hardening Coefficient [η] and Dimples Ratio [θ] values for the alloy at TT condition 150 °C/2h, for all diameters studied.

Table 3. (a) Elongation [δ]; (b) Strain Hardening Coefficient [η]; (c) Dimples Ratio [θ]for Al-0.05% Cu- [0.35-0.45]% Fe-0.22% Zr [TT 150 ° C / 2h], for all diameters.

Al-0.05% Cu- [0.35-0.45]% Fe-0.22% Zr [TT 150 °C/2h][(2)]			
Diameter wires [mm]	**Elongation [δ]**	**Strain Hardening Coefficient [η]**	**Dimples Ratio [ϑ]**
2.7	4.09	0.12	1.33
3.0	4.91	0.13	1.35
3.8	5.43	0.15	1.37
4.0	5.48	0.17	1.39

(1) Heat treatment at 150°C for 2 hours

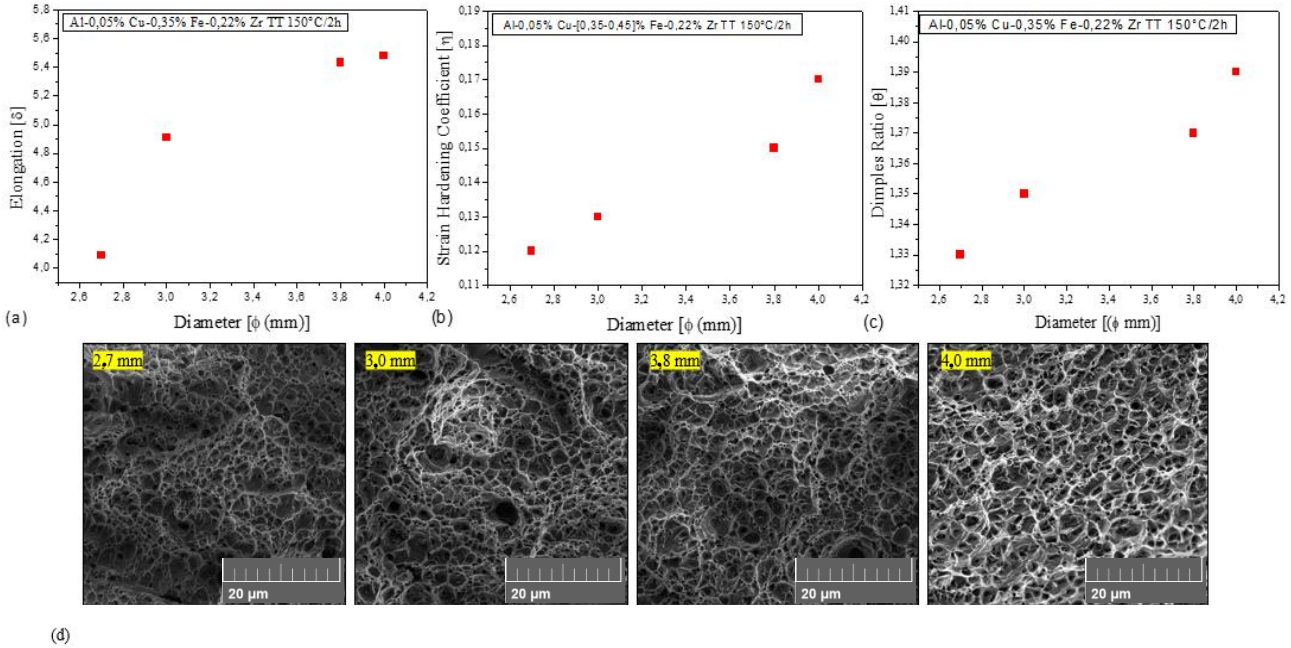

Figura 4. Ductility evaluation: (a) Elongation [δ]; (b) Strain Hardening Coefficient [η]; (c) Dimples Ratio [θ], for the alloy Al-0.05% Cu- [0.35-0.45]% Fe-0.22% Zr [TT 150 °C/2h], (d) for all diameters and associated with photomicrographs of the fractures for the diameter wires. Available from: GPEMat file.

3.3. Comparison of the results for the alloy under STT conditions and [TT 150 °C/2h]

The graphs in Figure 5 represent the comparison between the the Elongation [δ], Strain Hardening Coefficient [η] and Dimples Ratio [θ] values for STT alloy and heat after treatment. In addition, it correlates with the fractography of samples with a diameter of 3.00 mm.

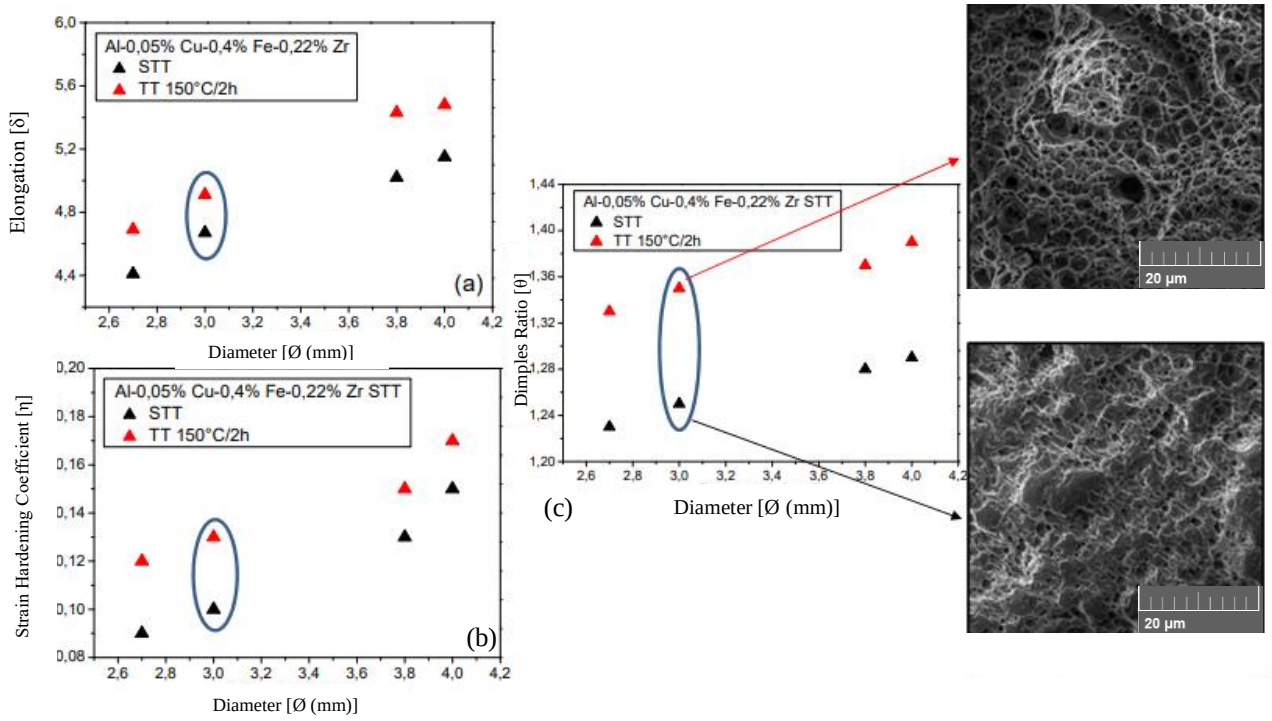

Figure 5. Comparison of (a) Elongation [δ]; (b) Strain Hardening Coefficient [η]; (c) Dimples Ratio [θ]for Al-0.05% Cu- [0.35-0.45]% Fe-0.22% Zr alloy under STT and [TT 150 ° C / 2h] conditions; for all diameters, associated with photomicrographs of fractures for 3.0 mm diameter wires. Available from: GPEMat file.

From the information set presented in 5, it can be inferred that the material in the condition [TT 150 ° C / 2h] presents gains in the values of Elongation [δ] and Dimples Ratio [ϑ]. This behavior indirectly shows that heat treatment improves the ductility ratio. Thus, there is a relationship between the increasing behavior of [η] and the increase in ductility. These factors are reflected in the photomicrographs of wire fractures. There are larger and more coalesced microcavities, associated with higher values of [δ], [ϑ] e [η].

On the other hand, the increasing behavior of UTS, previously observed for the heat treatment alloy, is generally associated with structures more mechanical hardening. It is possible that another factor is interfering with this behavior, making it important to analyze the [Stress] x [Strain] diagrams for further clarification.

3.4. Comparison of the curve [Stress] x [Strain] for STT and [TT 150 °C/2h]

The set of images in Figure 6 show the [Stress] x [Strain] diagrams for the alloys under the [STT] and [TT 150 °C/2h] conditions, cold deformed to the diameter 3.0 mm.

Initially, one should consider the probable conditions of the alloy structures, that is, the alloy in the STT condition, whose cooling occurred at a rate sufficient to prevent Zr diffusion, where the likely structural arrangement is a supersaturated solid solution Zr in Al. The alloy in the condition [TT 150 °C/2h], whose heat treatment temperature in the level of the biphasic region of the Al-Zr [α(Al)+Al_3Zr] diagram. This condition enables the formation of second phase particles in the form of Al_3Zr, which may precipitate from the supersaturated solid solution.

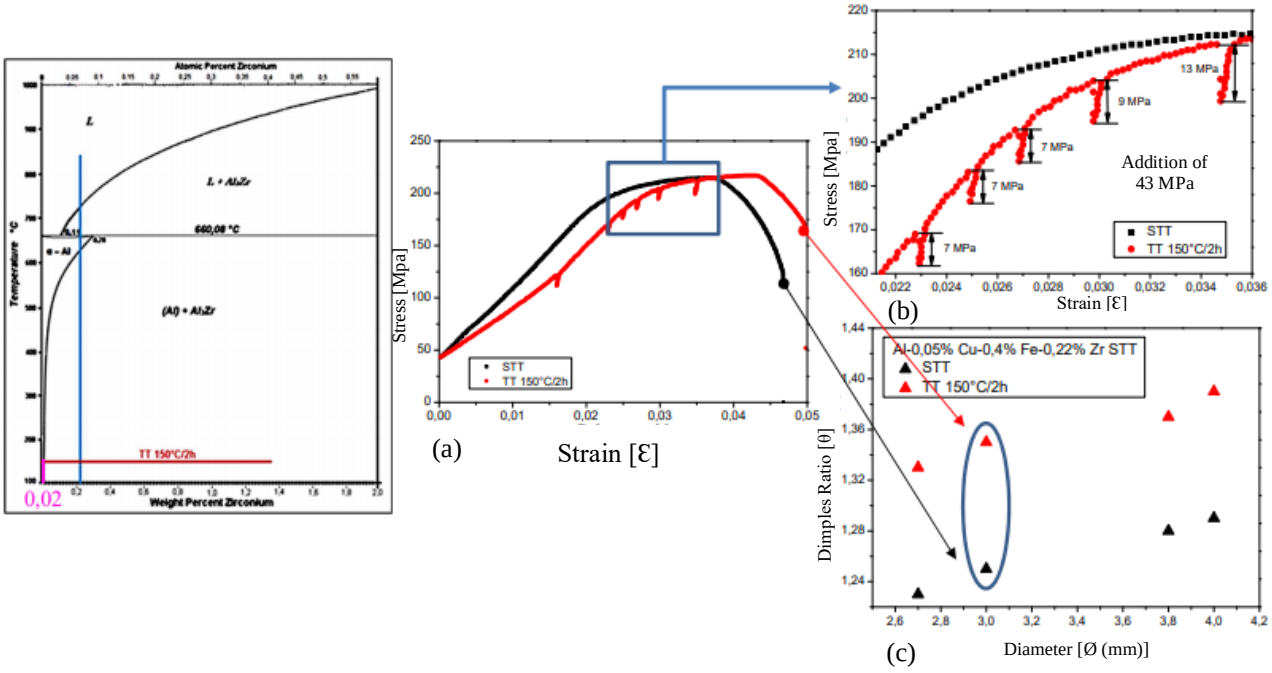

Figure 6. (a) and (b) Influence of the Portevin-Le Chatelier effect on the diagram [σ] x [ε] for the diameter 3.0 mm under STT and [TT 150 °C/2h] conditions; (c) Dimples Ratio [ϑ], with identification of the heat treatment temperature in the phase diagram Al-Zr. Available from: GPEMat file.

Regarding the particularities of each alloy, it can be evidenced that the heat treatment applied under the conditions of the present work is probably associated with the superplasticity phenomenon, more specifically with the Portevin-Le Chatelier effect [PLC]. which, in the treated alloy, increases in the yield resistance of the material, gradually, with the increase of 43 MPa. Such an effect delays the onset of narrowing, as illustrated by the region identified by the blue rectangle, resulting in larger and more coalesced microcavities.

On the other hand, the PLC effect is associated with the interaction between discordances and second phase particles. The occurrence of this phenomenon strongly suggests that during the heat treatment stage, the formation of second phase particles in the form of Al_3Zr may have occurred from the decomposition of the solid solution [α-Al], which act as anchorages efficient of discordances.

Given these considerations, it is likely that the increasing behavior of [η] is related to the possible precipitation of second phase particles [Al_3Zr], which apparently induce the material structure to superplasticity state.

4. CONCLUSION

The increasing behavior of Elongation [δ] and Dimples Ratio [ϑ] was found to be related to the increasing behavior of the Strain Hardening Coefficient [η], confirming that the alloy is gaining ductility with the application of heat treatment [TT 150 °C/2h]. Therefore, it is found that there is a relationship between [η] growth and increased ductility. These factors reflect the photomicrographs of wire fractures and tend to generate larger and more coalesced microcavities, associated with higher values of [δ], [ϑ] and [η].

Through this finding, it was performed the analysis of the diagrams [Stress] x [Deformation], observing that these variations may be related to the formation of second phase particles, which induce the phenomenon of superplasticity in the material. In addition, [PLC] causes, in the treated alloy, increased yield resistance of the material and delay in its narrowing.

5. ACKNOWLEDGEMENTS

At MSc. Marcos Cardoso for kindly giving in to the dissertation for writing articles and the Materials Engineering Research Group (MTERG).

6. REFERENCES

ASTM INTERNATIONAL, E 646. Standard Test Method for Tensile Strain-Hardening Exponents (n-Values) of Metallic Sheet Materials. Montgomery. ASTM International, 2000.

ASTM INTERNATIONAL, E 112. Standard Test Methods for Determining Average Grain Size. ASTM International, 2013.

BrasiL, "Ministério de Minas e Energia, Empresa de Pesquisa Energética. "Projeções da demanda de energia elétrica para o plano decenal de expansão de energia 2017-2026". Brasília: MME/EPE, 2017 < http://www.mme.gov.br/documents/10584/0/.../474c63d5-a6ae-451c-8155-ce2938fbf896>. Accessed on 21 March 2019.

Çadırlı, E., Tecer, H., Şahin, M., Yılmaz, E., Kırındı, T. and Gündüz, M., 2015. "Effect of heat treatments on the microhardness and tensile strength of Al–0.25 wt.% Zr alloy". *Journal of Alloys and Compounds*, Vol. 632, pp. 229-237.

Hu, Q. Zhang, Q., Fu, S., Cao, P. and Gong, M., 2011. "Influence of precipitation on the PortevinLe Chatelier effect in Al-Mg alloys". *Theoretical and Applied Mechanics Letters*, Vol. 1, n. 1.

Kamizono, K. A., 2014. Caracterização elétrica e mecânica da liga Al-Cu-Fe-Si modificada com os diferentes teores de ni para aplicação na fabricação de fios e cabos para transmissão e distribuição de energia elétrica. MS.C. dissertation, Universidade Federal do Pará, Belém, Brazil.

Knipling, K. E., Dunand, D. C. and Seidman, D. N., 2007. "Nucleation and precipitation strengthening in dilute Al-Ti and Al-Zr alloys". *Metallurgical and Materials Transactions A*, Vol. 38A, n. 10, pp. 2552-2563.

Mccormick, P. G., 1972. "A model for the Portevin-Le Chatelier effect in substitutional alloys". *Acta Metallurgica*, v. 20, n. 3, pp. 351-354.

Nagakrishna, N.; Akash, A.; Sivaprasad, K.; Narayanasamy, R., 2010. "Studies on void coalescence analysis of nanocrystalline cryorolled commercially pure aluminium formed under different stress conditions*". Materials & Design*, Vol. 31, n. 7, pp. 3578-3584.

Narayanasamy, R., Parthasarathi, N. L., Ravindran, R. and Narayanan, C. S., 2008. "Analysis of fracture limit curves and void coalescence in high strength interstitial free steel sheets formed under different stress conditions". *Journal of materials science*. Vol. 43, pp. 3351-3363.

NBR 6810, "Fios e cabos elétricos – Tração à ruptura em componentes metálicos". ABNT, Rio de Janeiro, 1981.

Polmear, I. et al. Light alloys: metallurgy of the light metals, 2017. 5. ed. Oxford: Butterworth-Heinemann.

Régis Jr, O., de Barros Bezerra, J.M., Domingues, L.A.C., Ueda, S. M. and Furukawa, C. U. C., 1999. "A utilização de condutores de liga de Al termo-resistente na repotencialização de LT de transmissão e sub-transmissão". In Seminário de Produção e Transmissão de Energia. Anais. Foz do Iguaçu, Brazil.

Sharma, V.M.J., Kumar, K.S., Nageswara Rao, B. and Pathak, S.D., 2009. "Effect of microstructure and strength on the fracture behavior of AA2219 alloy". *Materials Science and Engineering A*, Ed. 502, p. 45-53.

Soare, M. A., Curtin, W. A., 2008. Solute strengthening of both mobile and forest dislocations:the origin of dynamic strain aging in FCC metals. *Acta Materialia*, Vol. 56, n. 15, pp. 4046–4061.

7. RESPONSIBILITY NOTICE

The authors are the only responsible for the printed material included in this paper.